BEHAVIOR OF COMPOSITE/METAL AIRCRAFT STRUCTURAL ELEMENTS AND COMPONENTS UNDER CRASH TYPE LOADS--WHAT ARE THEY TELLING US?

Huey D. Carden*
NASA Langley Research Center
Hampton, VA

Richard L. Boitnott**
U.S. Army Aerostructures Directorate, AVSCOM
Langley Research Center
Hampton, VA

Edwin L. Fasanella†
Lockheed Engineering and Sciences Company
Hampton, VA

Abstract

Failure behavior results are presented from crash dynamics research using concepts of aircraft elements and substructure not necessarily designed or optimized for energy absorption or crash loading considerations. To achieve desired new designs which incorporate improved energy absorption capabilities often requires an understanding of how more conventional designs behave under crash loadings. Experimental and analytical data are presented which indicate some general trends in the failure behavior of a class of composite structures which include individual fuselage frames, skeleton subfloors with stringers and floor beams but without skin covering, and subfloors with skin added to the frame-stringer arrangement. Although the behavior is complex, a strong similarity in the static/dynamic failure behavior among these structures is illustrated through photographs of the experimental results and through analytical data of generic composite structural models. It is believed that the similarity in behavior is giving the designer and dynamists much information about what to expect in the crash behavior of these structures and can guide designs for improving the energy absorption and crash behavior of such structures.

Introduction

The NASA Langley Research Center has been involved in crash dynamics research since the early 1970's. For about the first 10 years the emphasis of the research was on metal aircraft structures during the General Aviation Crash Dynamics Program [1 - 13] and a transport aircraft program, the Controlled Impact Demonstration (CID), which culminated with the remotely piloted crash test of a B-720 aircraft [14 - 16] in 1984. Subsequent to the transport work, the emphasis has been on composite structures with efforts directed at developing a data base of understanding of the behavior, responses, failure mechanisms, and general loads associated with the composite material systems under crash loadings. (See Figure 1). Considerable work has been conducted into determining the energy absorption characteristics [17 - 20] of composites. These results indicated that composites can absorb as much if not considerably more energy than comparable aluminum structures. However, because of the brittle nature of the materials, attention must be given to proper geometry and designs which will take advantage of the good energy absorbing properties while at the same time providing desired structural integrity during normal flight loading conditions. To achieve the desired new designs often requires an understanding of how more conventional designs behave under crash loadings.

The purpose of this paper is to present an overview of the research conducted using concepts of aircraft elements and substructure which have not necessarily been designed or optimized for energy absorption or crash loading considerations. Experimental and analytical data are presented which indicates some general trends in the failure behavior of a class of composite structures which include individual fuselage frames, skeleton subfloors with stringers and floor beams but without skin covering, and subfloors with skin added to the frame-stringer arrangement. Although the behavior is complex, a strong similarity in the static/dynamic failure behavior among these structures is illustrated through photographs of the experimental results and through analytical data of generic composite structural models. It is believed that the similarity in behavior is giving the designer and dynamists much information about what to expect in the crash behavior of these structures and can guide designs for improving the energy absorption and crash behavior of such structures.

Impact Dynamics Research Facility

The information presented in this report is the result of a research program to investigate the impact response of transport and composite aircraft components conducted at the NASA Langley Research Center's Impact Dynamics Research Facility (IDRF). The IDRF (shown in figure 2) is the former Lunar Landing Facility used to train astronauts for moon landings. The facility is 220 feet high and 400 feet long. In the early 1970's, the structure was converted for crash testing of full-scale general aviation aircraft. Reference 21 provides complete details of the facility and test techniques for full-scale aircraft testing. Additionally, a photograph of a 70 foot high Vertical Drop Test Apparatus often used for full-scale aircraft section, components, and/or seat testing is shown in Figure 3. Static testing machines, and other apparatus are also available at the facility for metal and composite aircraft structural testing.

Analysis Tools

To gain an understanding of fundamental physical behavior of complex structures, the experimental research with structures under crash loadings is generally accompanied by analytical prediction/correlation studies whenever feasible. Thus, various finite element codes which have capabilities for handling dynamic, large displacement, nonlinear response problems of metal and composite structures are used as tools in the various research efforts.

---

* Assistant Head, Landing and Impact Dynamics Branch
**Research Engineer
† Staff Engineer

DYCAST Computer Code

The analytical results presented in this overview were generated with a nonlinear finite element computer code called DYCAST (DYnamic Crash Analysis of STructures)[22] developed by Grumman Aerospace Corporation with principal support from NASA and FAA. The basic element library consists of (1) stringers with axial stiffness only; (2) beam elements with 12 fixed cross-sectional shapes typical of aircraft structures with axial, two shear, torsional, and two bending stiffnesses; (3) isotropic and orthotropic membrane skin triangles with membrane and out-of-plane bending stiffnesses;(4) isotropic plate bending triangles with membrane and out-of-plane bending stiffnesses; and (5) nonlinear translational or rotational spring elements that provide stiffness with user-specified force-displacement or moment-rotation tables (piece-wise linear). The spring element can be either elastic or dissipative. The springs are useful to model crush behavior of components for which experimental or analytical data are available and/or whose behavior may be too complex or time consuming to model otherwise. An effort is underway to add curved composite beams, composite plate, and curved shell elements to the DYCAST element library.

Test Specimens and Description

Full-Scale Metal Aircraft Structures

NASA Langley Research Center conducted three vertical drop tests of metal aircraft sections to support transport aircraft research efforts. Selected data on the crash behavior of full-scale metal transport aircraft sections[23 - 24] are included in the present paper to demonstrate what appears to be important similarities in behavior noted for both the metal fuselage structures and the composite structures discussed herein.

Two 12-foot long fuselage sections cut from an out-of-service Boeing 707 transport aircraft were drop tested to measure structural, seat and occupant responses to vertical crash loads, and to provide data for nonlinear finite element modeling. One fuselage section was cut from forward and one was cut from aft of the wing location of the aircraft . A photograph of the forward section suspended in the Vertical Drop Test Apparatus at the Impact Dynamics Research Facility is shown in Figure 4. The aft section tests served two purposes: 1) to test structural, seat, and anthropomorphic dummies response , and 2) to test the data acquisition system pallet, power pallet, and camera batteries and instrumentation later used in the full-scale transport crash program. The reader should refer to the particular reports [14-16] and [23-24] for more complete descriptions of the test articles since such information is not repeated in this report.

Composite Structures

Single Composite Frames.- Various cross-sectional shapes for fuselage frames are used in metal aircraft and are often proposed for composite structures. Sketches and photographs illustrating four of the more common geometries, I-, J-, C- and Z-cross sectional shapes are shown in Figure 5 (a), (b) and (c). Several circular frames with these shapes were fabricated for testing to add to the composite structures data base . To add out-of-plane stability to the frame concepts (with the exception of the Z-section frames), 2 1/4 or 3 1/2 inch wide skin material was added which enhanced the ease of testing of both symmetrical and nonsymmetrical cross-sections. The .08 inch thick, sixteen ply skin, with a $[\pm 45/0/90]_{2s}$ lay-up was co-cured with the 6 foot diameter frames which have the lay-ups as indicated in Table I. The frame cross-sections were constructed in two different heights, 1 1/2 inches high and 3/4 inches high, to investigate the effect of frame height on behavior and responses.

Table I.- Composite frame section lay-ups.

Fuselage Frame Label	Serial Number	Configuration	Lay-up	Weight (Kg)
FR004I	1	I-section	$(\pm 45/0/90)_s$	1.443
FR005I	1	I-section	$(\pm 45/0/90)_{2s}$	1.996
FR004J	2	J-section	$(\pm 45/0/90)_{2s}$	1.853
FR005C	1	C-section	$(\pm 45/0/90)_{2s}$	1.229
FR005C	2	C-section	$(\pm 45/0/90)2s$	1.229

One of the first geometries to be studied under static and dynamic loadings was the Z-cross section. A photograph of Z-cross section fuselage frames used in the initial studies of the behavior of composite structural elements under impact loads is shown in Figure 5(c). A Z-frame suspended in the drop apparatus prior to testing is shown in Figure 6. The apparatus was constructed with guide rails, a rear metal backstop, and a front plexiglas sheet. During free-fall the specimen was guided and the front and rear backstops prevented some (but not all) out-of-plane bending or twisting during impact, and allowed photographs and motion picture coverage through the front plexiglas plate . The six-foot diameter frames were constructed using a quasi-isotropic lay-up of 280-5HA/3502, a five harness satin weave graphite fabric composite material. The Z-cross section of the frame was 3 inches high with a total width of 2.25 inches and about 0.08 inches thick. Initial tests were with 360 degree frames made from four 90 degree segments joined with splice plates as shown in figure 5(c). Additional tests were conducted with half frames since the top half of the complete frames were undamaged in the tests.

The approach of studying simple structural elements and then moving to combinations of these elements into more complex substructures has been taken in the development of a data base on the dynamic response and behavior of composite aircraft structures. The approach parallels the one used during the general aviation and transport aircraft programs. Consequently, three composite subfloor structures were fabricated following the initial investigation of the Z-frames discussed above.

Subfloor Structures.- A photograph of the skeleton and skinned subfloor specimens constructed with three of the single Z-section frames similar to those that were studied earlier is shown in Figure 7. Pultruded J-stringers connected the three frames through metal clips and secondary bonding methods. Aluminum floor beams tied the top diameter of the frames together to form the lower half of the subfloor. Notches in the frames allowed the stringers to pass through the frames. Two subfloors without skin (called skeleton subfloors) were fabricated. A third specimen (called skinned subfloor) had a ±45 lay-up skin bonded and riveted to the frames to form the lower fuselage structure.

Full-Scale Composite Aircraft.- Two full-scale composite general aviation aircraft structures, two complete wing sets, and landing gears have been obtained for testing. Because of the scarcity and expense associated with obtaining full-scale composite aircraft for impact testing, plans include multiple usage of the structures. Various structural, and impact tests will provide additional information for the composites data base.

Results and Discussion

Experimental and analytical results from the studies of full-scale aircraft structures, composite fuselage frames, and subfloors under static and/or dynamic loadings are presented in Figures 8 to 18. Photographs are included which emphasize the failure behavior of the composite and metal aircraft components and show a strong similarity in their behavior. The behavior is thought to be an important aspect which must be considered in the design of new structures for improving the energy absorption and crash behavior of these type components and structural elements.

Full-Scale Metal Aircraft Structures

Experimental and analytical results from studies with full-scale transport category aircraft sections [23 - 24] are presented in figure 8.

Dynamic tests.- Structural damage of the transport aircraft structures resulting for the 20 ft/s drop tests is shown in figure 8(a) and (b). The damage to the transport sections was confined to the lower fuselage below the floor level. Under the vertical impact of 20 ft/s, all seven of the frames ruptured near the bottom impact point. Plastic hinges formed in each frame along both sides of the fuselage about 50 degrees up the circumference from the bottom contact point (See figure 8(c)). The crush of the lower fuselage was approximately 22-23 inches at the front end and 18-19 inches at the rear for the section taken from forward of the wing location (figure 8(a)) whereas for the aft section (figure 8(b)) the crushing was about 14 inches in front and 18 inches in the rear. Although the aircraft structures are metal and the failures discussed above involve plastic deformations with some tearing of the metal rather than brittle fractures, the general observed failure pattern and locations for the transport fuselage sections will be shown to be quite similar to the results of the composite frames and subfloors discussed later.

Analytical studies.- A DYCAST model of the section (from forward of the wing location) was constructed to model the floor, two seats with lumped mass occupants, and the fuselage structure to determine if such a model could predict the response of the complete section with fidelity. The finite element model is shown in figure 9. Stiff ground springs simulated the concrete impact surface. Each frame of the fuselage below the floor was modeled with eight beam elements and floor and seat rails were also appropriate beam elements. Fuselage structure above the floor (not expected to fail) was modeled in less detail.

A comparison of the two frame analytical predictions and the full section experimental responses are shown in figure 10. The correlation of the vertical displacement, wall/floor, and dummy pelvis accelerations are considered good. As may be noted in figure 10(d), the overall impression from the analytical model deformation pattern is quite similar to the visual behavior seen in the experiment shown in figure 8. Thus, the full section behavior was basically contained in the two frame model.

In the following sections the composite impact dynamics studies have taken the building block approach of utilizing a sequence of testing and analysis which begins with 'simpler' elements and move to more 'complicated' components or substructures. As mention earlier, this approach was used in the General Aviation (GA) and Transport programs although the GA data base was being concurrently developed through full-scale testing. Full-scale tests using currently available composite aircraft specimens and/or other full-scale structures are part of the on-going research program.

Full-Scale Composite Aircraft

Other than two support tests for Army composite aircraft programs[25-26], no testing of full-scale composite aircraft has been conducted at the Langley Research Center as part of the composite impact dynamics research. However, as indicated previously, composite aircraft fuselage specimens have been obtained for crash testing.

Composite Single Frame Studies

Static tests.- Results from the static test of a semi-circular frame with a Z cross-section[27] are presented in Figure 11. A photograph of the static test apparatus in figure 11(a) shows that the splice plate was at the load point. Consequently, the frame failed just outside the doubler splice plate area by a complete fracture across the Z-section. Load-deflection data and the location of failures of the frame are shown in figure 11(b). The load-deflection data show a saw-toothed behavior of loading and unloading. The load increased linearly until initial failure, then falls off to under 600 pounds force. Subsequent loading of the frame after initial failure was at a new, reduced stiffness. Second and third fractures occurred up the side again at about 54 and 58 degrees under continued loading as may be noted in the sketch at the right of figure 11(b). Photographic data in figure 10(c) shows that the initial failure was induced by a local buckling of the frame which occurred at about 18 degrees from the bottom loading point outside the splice plate area.

Static analytical studies.- To demonstrate analytically the apparent behavior of the frames under load (exclusive of the local buckling which actually initiated the failure in the static case), two DYCAST finite-element models were constructed. For ease of analysis, a typical I-section was modeled from the specimens described in the "Single Frame Studies" section. The frame was loaded at the top and a simulated ground plane (ground contact springs) resisted the vertical movement of the frame during load application. Only half the frame was modeled using thirty-four (34) I-section beam elements with boundary conditions imposed at the bottom node of the model to account for the symmetrical situation. The top node was constrained to allow only vertical displacement thus simulating the effect of a very stiff floor across the frame diameter. The static load was slowly increased until an input failure strain for the material (0.0086) was exceeded at the point of loading and failure was indicated. The curve labeled *unbroken frame, case I,* in figure 12(a) is the load-deflection plot for this case I.

A second DYCAST model, *broken frame, case II,* was also run wherein the bottom point of the frame was modeled with two short skin segments to represent the different boundary condition following the initial failure of the frame. This condition will be discussed further relative to the composite subfloor test with the skinned subfloor specimen. The curve in figure 12(a) labeled *case II* is the load-deflection response for this frame loading case. Essentially, the frame load increases along the *case I* curve to the point of initial failure at the bottom of the frame. After the frame fractures the boundary changes to one considerably weakened--down to the bending stiffness of the skin alone at that location. The load then drops to the lower curve, *case II,* which represents the stiffness of the section with the weakened boundary on the bottom end of the frame. The load continues to increase along the *case II* curve until secondary failures at some other location on the frame circumference occur.

An examination of the normalized distribution of the bending moment on the frame shown in figure 12(b) provides insight and a better understanding of the failure/behavior. Maximum moments are indicated (just prior to failure) to be at the 0 degree location and between ±50-60 degrees from the bottom contact area. The locations correlate well with the failure locations in the experiment with the Z-frame.

Normalized bending moment distribution on the broken frame is presented in Figure 12(c). As may be noted, the distribution is quite similar to the initial model results in figure 12(b). The failure location is at the maximum bending moment location predicted to be about ±45 degrees which is somewhat lower than the same location shown in the initial model of the unbroken frame. The agreement between the predicted behavior by the two models, however, is still considered good. The effect of diameter on the moment distribution of the frame was assessed with a model having a 75 inch diameter (twice the initial diameter). The distribution was identical to the smaller diameter results, however, the loads producing the moments differed between the two models (as expected). Moment in terms of geometry and load for a point loaded ring[28] shows that the maximum moment will occur at the same angle for different values of diameter.

Furthermore, a comparison of the analytical cases (figure 12(a)) with the actual static load-deflection of the Z-section (figure 11(b)) indicates very similar load-deflection behavior patterns as discussed above. Although the Z-frame had no skin, if the ends jam together (as they did in several cases), the boundary is effectively between the skin stiffened case and a guided boundary. Thus, the predicted maximum moment location in the simple beam-frame model at about 50 degrees (See figure 12(b)) agrees well with the 54 and 58 degree failure locations in the experiment with the Z-section frame.

Without a priori knowledge of the manner of the failure noted and discussed above, the initial formulation of a finite-element model would unlikely incorporate the necessary failure mechanism/behavior for the frames. However, knowing the pattern of behavior can enable the analyst to formulate adequate finite-element models to predict dynamic responses including the failure/loads. Additionally, such information is important to designers of new structures to be able to design for impact loads on such structural elements of an aircraft fuselage.

Dynamic tests.- Results from reference 29 on the dynamic studies of the response of composite frames are shown in Figure 13. Photographs of the failed Z-frames in the drop apparatus are shown in Figure 13(a). It should be noted, the splice plates joining the segments of the frame are 45 degrees up the circumference from the point of impact. As shown in figure 13(b), complete failures (fractures) of the Z-section frames occurred at the bottom and approximately 60 degrees from the bottom. It appears that the presence of the splice plates moved the top failure points up a few degrees (to about the 60 degree locations).

Dynamics analytical studies.- Experimental and analytical model results for the composite Z-frame subjected to a 20 ft/s impact are shown in Figure 13(c). The first 15 milliseconds of the experimental acceleration of the floor and analytical predictions are shown. In one analysis, in-plane deformations were constrained to the plane of the frame whereas in the other, the frame was free to twist and bend out-of-plane. As noted in the figure, agreement between the "free" model and the experiment is good for the initial peak load. Later the agreement is less because the backstop and clear fence in the experiment, which was not modeled, began to provide support to the twisting and bending frame. The in-plane model results are about 60% higher when compared to the experiment and the free model results. Such results emphasize the importance of knowing and modeling the experimental boundary conditions to understand the dynamic and static behavior of structures under crash loadings. Unfortunately, mixed boundary conditions often exist or occur in the experiments.

Composite Subfloor Studies

Two static and two dynamic tests were conducted on the three composite subfloor specimens used for impact studies. Two skeleton subfloor were tested to destruction, one statically and the other dynamically. The skinned subfloor was subjected to a non-destructive static test followed by a dynamic test to failure.

Static tests.- Experimental results[30] of the skeleton subfloor specimen following a static test are shown in Figure 14. As noted in figure 14(a) and (b), failures on the three Z-section frames occurred at 13 discrete locations. Unlike the unnotched single Z-frame, the failures in this specimen occurred at notches (which served as stress risers) in the frame through which the stringer passed. However, as shown in figure 14(b) the failures were still near the point of load application (approximately 11 degrees) and at other circumferential locations of approximately 45 to 67 degrees. In the absence of skin material, twisting and bending out-of-plane occurred with the frames. The stringers had only a minimal effect on the subfloor response and that was to maintain the lateral spacing of the three Z-frames.

Dynamic tests.- A photograph of a skeleton subfloor after an impact test onto a concrete surface at 20 feet per second is shown in Figure 15. In the dynamic test of the skeleton subfloor, fractures were produced at notches in the frames (Figure 15(a)). The locations, shown in figure 15(b), were also near the point of impact (about 11 degrees because of the splice plate) and at three other locations up the circumference of the frames (55 degrees and 78 degrees) totalling 15 fractures for all three frames. The impact energy exceeded the energy absorbed by the local fractures and the floor bottomed out during the impact. The normalized circumferential strain distribution measured on the flange of the front frame during the dynamic test just before first failure is shown in Figure 15(c). A comparison of the measured distribution to the predicted moment distribution of Figure 12(b) and (c) shows essentially identical shape between the single frame and skeleton frame distributions. Maximum values at 0 degrees and at approximately 50 to 55 degrees for the experiment agree well with the analytically predicted locations on the frame.

Impact results for the subfloor with skin after an impact of 20 feet per second are shown in Figure 16. A photograph of the subfloor specimen after the test is shown in Figure 16(a). Points of failure of the frames in this specimen are indicated in figure 16(b). Again the points of failure are at or near the impact point (within 12 degrees) and circumferentially at about 56 degrees up both sides of the frame on the middle and back frame and 45, 12 and 22.5 degrees on the front frame. It was observed that the subfloor impacted first on the front area which possibly explains the 12 and 22.5 degree fractures being different from the other locations. Again all three frames were involved in the failures. Some delamination of the frames from the skin was evident but the skin remained intact. Normalized strain distribution (just prior to first failure) measured on the skin at the location of the front frame during the dynamic test showed essentially identical shape as the single frame and skeleton frame distributions. As was the case for the skeleton subfloor maximums at 0 degrees and at approximately 50 to 55 degrees for the experiment agree well with the analytically predicted locations on the frame.

As mentioned previously in the frame studies, once the frames fail at/near the point of impact the broken ends of the frame often jammed together and moved upward in a guided manner. In the subfloor structure, the frames may still fail completely across the section but the skin remains intact and serves as a much less stiff boundary condition for the broken frames as the deflection increases. Little energy is involved in

skin snap-through as the load increases on the structure (See reference 31 on snap-through of composite arches). In this manner, the structural stiffness of the frame/skin before fracture changes to the skin only after frame fracture. The analytical models discussed herein simulated this type of behavior.

Analytical studies.-The contribution of the skin to the stiffness of the section with the nonsymmetrical frames is illustrated in figure 17. Static load-deflection data for the unskinned subfloor and the skinned subfloor along with the DYCAST predictions are shown in the figure. It can be noted that the subfloor stiffness (with skin) is approximately three times the stiffness of the skeleton subfloor, thus the skin's contribution to the structure is to maintain in-plane deflections of the non-symmetrical Z-section and prevent any substantial twisting of the frames. Out-of-plane bending and twist were allowed in the skeleton subfloor predictions.

General Observations

The response behavior determined during the studies of full-scale aircraft sections, fuselage frames, and subfloors are summarized in figure 18. Normalized moment distribution on a representative frame of the various specimens are shown in Figure 18(a). Figure 18(b) shows the failure locations which were noted from static and dynamic tests. The visual impression is quite striking among the various specimens. The structures all share in common the generally circular or cylindrical shape, the normal loading situations, and what appears to be a similar pattern of failure behavior. Analytical models of frame structures under vertical loads have moment distributions which have maximums at the point of loading and at approximately 45 to 50 degrees (depending on boundary conditions) around the circumference from the ground contact point. Failures of the structures were noted at these same locations. Such observations may help dynamists gain a clearer understanding of what to expect from such structures in crash loading situations, may guide designers of new structures to account for the vertical crash loads, and allow increased energy absorption to be included in the new designs. Additionally, the observations may help analysts to model the aircraft structures more adequately for predicting the failure responses and behavior under crash situations. The latter task is a difficult and challenging one, not only for composite structures but for metal structures as well. Studies are currently underway to improve the analysis capabilities of current codes and to add composite elements to finite element libraries such as the DYCAST program. In addition, new analysis approaches are being explored through grants to universities as an extension of NASA Langley Research Center's in-house efforts.

Concluding Remarks

Some important failure behavior results from the research with composite full-scale aircraft sections, composite structural elements, and subfloors have been presented. Observations of the failure behavior of these structures have been made and discussed and analytical results have been included to help explain some of the behavior noted.

From the research presented in the overview the following conclusions are made:

(1) Comparing the results from simple representative structural elements with more complex components provided insight into the the local/global structural responses and behavior of complex aircraft structures.

(2) Relatively simple analytical models provided generally good correlation with experiments; however, guidance from experimental data was required to allow adequate or improved analytical models to be formulated.

(2) Commonality in the failure behavior patterns among full-scale aircraft sections, composite frames, and subfloors with and without skin was found.

(3) General locations of failures appear to occur at the same structural regions among the specimens as a result of similar geometry, similar loading, and similar moment distribution on the structures under vertical loads.

(4) Noted failures were located in the same regions as the maximums in the moment distribution on the structures.

(5) The shape of the distribution of the moment was independent of the diameter of the frame/component. Loads, however, which produced the failures varied with the structural size.

Concluding Observations

Based upon the conclusions drawn from the various research efforts discussed in this paper, the following observations are also summarized:

(1) The general similarity of the failure behavior among the aircraft structures can:

(a) assist the designer and dynamists to anticipate how the structures probably will fail,

(b) provide guidance on how and where to incorporate and/or optimize improved energy absorption into new aircraft structural designs, and

(c) aid analysts to more adequately model the structures for predicting failure/loads behavior under crash situations.

(2) To analytically predict, in a dynamic loading situation, the complex failure events and the loads which initiate the failures as noted in the composite structural elements and sub-components is a challenge, but possible; however, guidance is often required from experiments.

(3) Composite curved beam, composite plate and shell elements are being developed and included in finite-element codes to improve the capability to analyze composite structures.

References

1. Alfaro-Bou, Emilio; and Vaughan, Victor L., Jr.: Light Airplane Crash Tests at Impact Velocities of 13 and 27 m/sec. NASA TP 1042, November 1977.

2. Castle, Claude B.; and Alfaro-Bou, Emilio: Light Airplane Crash Tests at Three Flight-Path Angles. NASA TP 1210, June 1978.

3. Hayduk, Robert J.: Comparative Analysis of PA-31-350 Chieftain (N44LV) Accident and NASA Crash Test Data. NASA TM 80102, October 1979.

4. Castle, Claude B.; and Alfaro-Bou, Emilio: Light Airplane Crash Tests at Three Roll Angles. NASA TP 1477, October 1979.

5. Vaughan, Victor L., Jr.; and Alfaro-Bou, Emilio: Light Airplane Crash Tests at Three Pitch Angles. NASA TP 1481, November 1979.

6. Vaughan, Victor L., Jr.; and Hayduk, Robert J.: Crash Tests of Four Identical High-Wing Single-Engine Airplanes. NASA TP 1699, August 1980.

7. Carden, Huey D.; and Hayduk, Robert J.: Aircraft Subfloor Response to Crash Loadings. SAE Paper 810614, April 1981.

8. Williams, M. Susan; and Fasanella, Edwin L.: Crash Tests of Four Low- Wing Twin-Engine Airplanes with Truss-Reinforced Fuselage Structure. NASA TP 2070, September 1982.

9. Carden, Huey D.: Correlation and Assessment of Structural Airplane Crash Data with Flight Parameters at Impact. NASA TP 2083, November 1982.

10. Carden, Huey D.: Impulse Analysis of Airplane Crash Data with Consideration Given to Human Tolerance. SAE Paper 830748, April 1983.

11. Castle, Claude B.; and Alfaro-Bou, Emilio: Crash Tests of Three Identical Low-Wing Single-Engine Airplanes. NASA TP 2190, September 1983.

12. Thomson, Robert G.; Carden, Huey D.; and Hayduk, Robert J.: Survey of NASA Research on Crash Dynamics. NASA TP 2298, April 1984.

13. Carden, Huey D.: Full-Scale Crash Test Evaluation of Two Load-Limiting Subfloors for General Aviation Airframes. NASA TP 2380, December 1984.

14. Hayduk, Robert J.(Editor): Full-Scale Transport Controlled Impact Demonstration. NASA CP 2395, April 1985.

15. Fasanella, Edwin L.; Widmayer, E.; and Robinson, M. P.: Structural Analysis of the Controlled Impact Demonstration of a Jet Transport Airplane. AIAA Paper 86-0939-CP, May 1986.

16. Fasanella, Edwin L.; Alfaro-Bou, Emilio; and Hayduk, Robert J.: Impact Data from a Transport Aircraft During a Controlled Impact Demonstration. NASA TP 2589, September 1986.

17. Farley, Gary L.: Energy Absorption of Composite Materials. NASA TM 84638, AVRADCOM TR-83-B-2, 1983.

18. Bannerman, D.C.; and Kindervater, C.M.: Crashworthiness Investigation of Composite Aircraft Subfloor Beam Sections. IB 435-84/3(1984), Deutsche Forschungs- und Versuchasanstalt fur Luft-und Raumfarht, February 1984.

19. Cronkhite, J.D.; Chung, Y.T.; and Bark, L.W.: Crashworthy Composite Structures. ASAAVSCOM TR-87-D10, U.S. Army, December 1987. (Available from DTIC as AD B121 522.)

20. Jones, Lisa E.; and Carden, Huey D.: Evaluation of Energy Absorption of New Concepts of Aircraft Composite Subfloor Intersections. NASA TP 2951, November 1989.

21. Vaughan, Victor L.; and Alfaro-Bou, Emilio: Impact Dynamics Research Facility for Full-Scale Aircraft Crash Testing. NASA TN D-8179, April 1976.

22. Pifko, A.B.; Winter, R.; and Ogilvie, P.L.: DYCAST - A Finite Element Program for the Crash Analysis of Structures. NASA CR 4040, January 1987.

23. Williams, M. Susan; and Hayduk, Robert J.: Vertical Drop Test of a Transport Fuselage Section Located Forward of the Wing. NASA TM 85679, August 1983.

24. Fasanella, Edwin, L.; and Alfaro-Bou, Emilio: Vertical Drop Test of a Transport Fuselage Section Located Aft of the Wing. NASA TM 89025, September 1986.

25. Cronkhite, James D.; and Mazza, L.T.: Bell ACAP Full-Scale Aircraft Crash Test and KRASH Correlation. American Helicopter Society, 44th Annual Forum and Technology Display, Wash. D.C., June 1988.

26. Cronkhite, James D.; and Mazza, L.T.: KRASH Analysis Correlation with the Bell ACAP Full-Scale Aircraft Crash Test. American Helicopter Society National Specialists' Meeting on Advanced Rotorcraft Structures, Williamsburg, Va., October 1988.

27. Boitnott, Richard L.; and Kindervater, Cristof: Crashworthy Design of Helicopter Composite Airframe Structure. Fifteenth European Rotorcraft Forum, Amsterdam, Holland, Paper Nr; 93, September 1989.

28. Van Den Broek, J.A.: Elastic Energy Theory. 2nd Edition, John Wiley and Sons,Inc., New York, August 1946, pp. 100-104.

29. Boitnott, Richard L.; Fasanella, Edwin L.; Calton, Lisa E.; and Carden, Huey D.: Impact Response of Composite Fuselage Frames. SAE Paper 871009, April 1987.

30. Boitnott, Richard L.; and Fasanella, Edwin L.: Impact Evaluation of Composite Floor Sections. SAE Paper 891018, General Aviation Aircraft Meeting and Exposition, Wichita, Kansas, April 1989.

31. Carper, Douglas M.; Hyer, Michael W.; and Johnson, Eric R.: Large Deformation Behavior of Long Shallow Cylindrical Composite Panels. Virginia Polytechnic Institute and State University, VPI-E-83-37, September 1983.

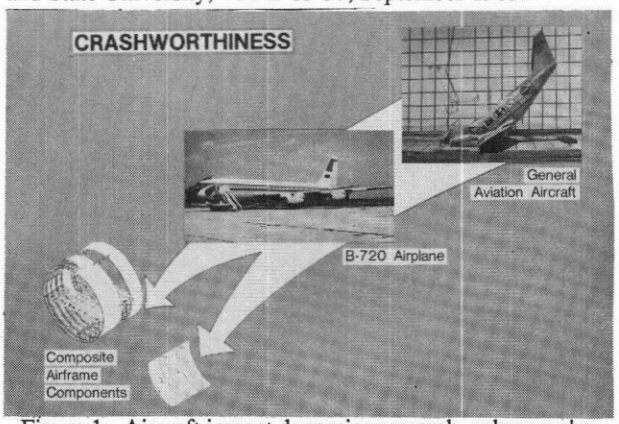

Figure 1.- Aircraft impact dynamics research--where we've been, where we're going.

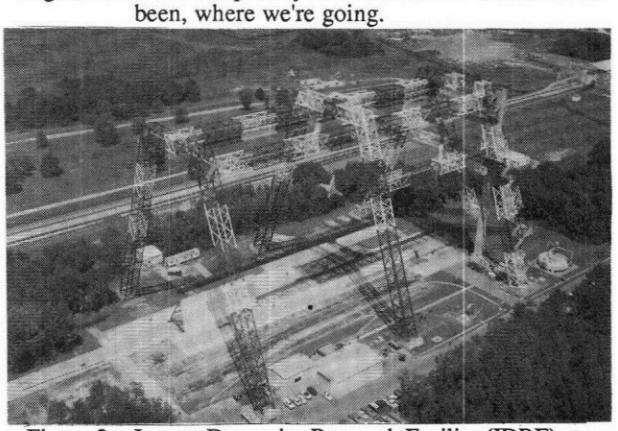

Figure 2. - Impact Dynamics Research Facility (IDRF) at NASA Langley Research Center.

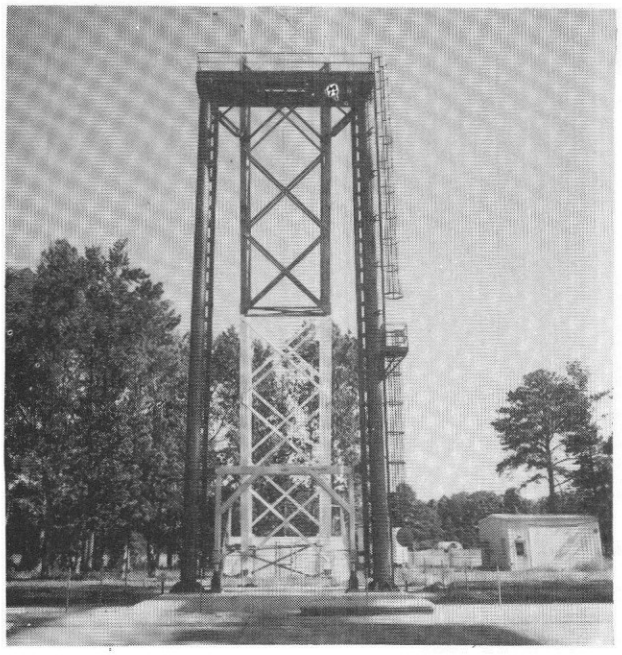

Figure 3. - Vertical Drop Test Apparatus used in testing of aircraft sections and components.

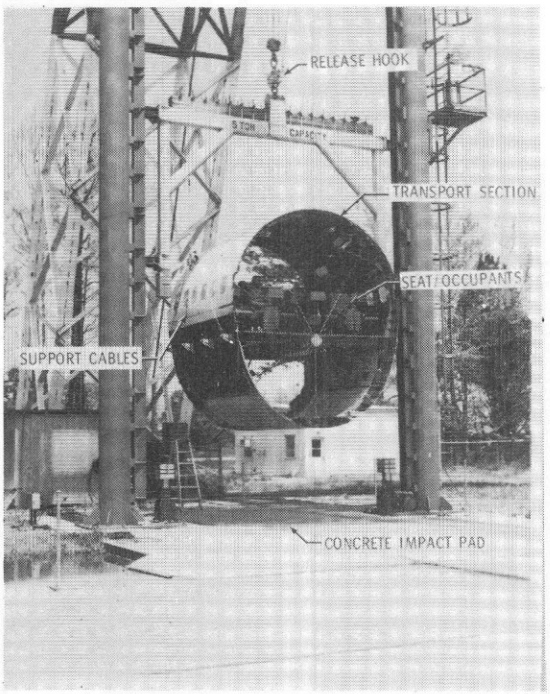

Figure 4. - Metal transport section suspended in Vertical Test Apparatus.

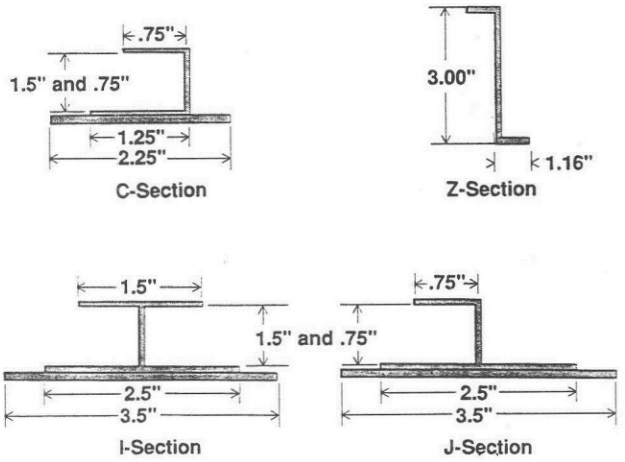

(a) Cross-sectional dimensions.

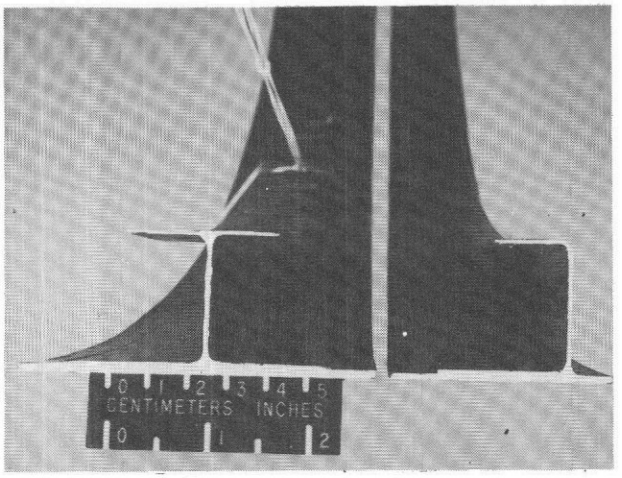

(b) I and C section frames.

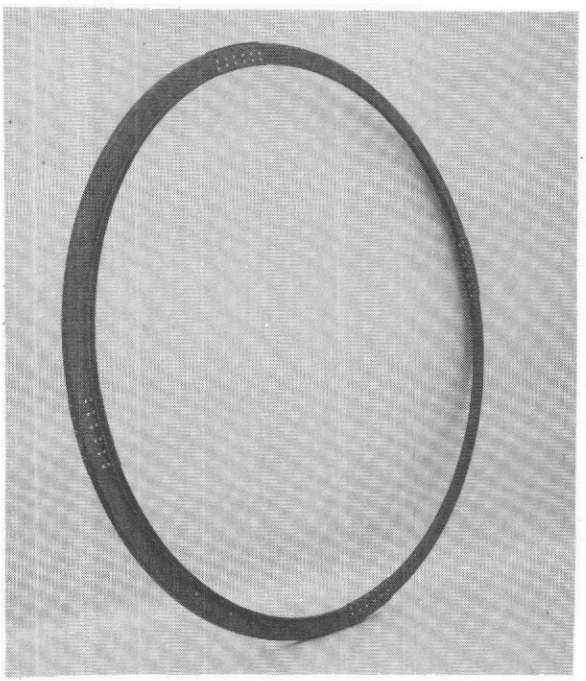

(c) Z-cross section fuselage frame.

Figure 5. - Various cross-sectional shapes of composite fuselage frames.

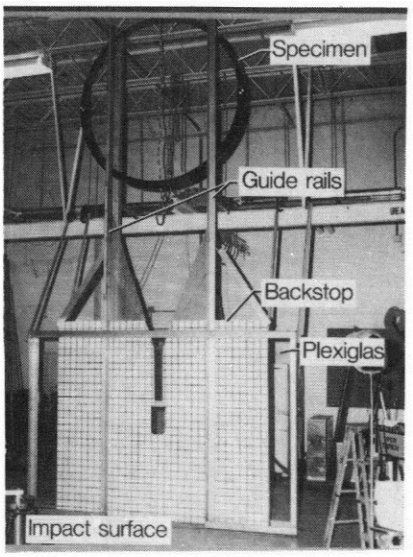

Figure 6. - Composite Z-frame in drop apparatus.

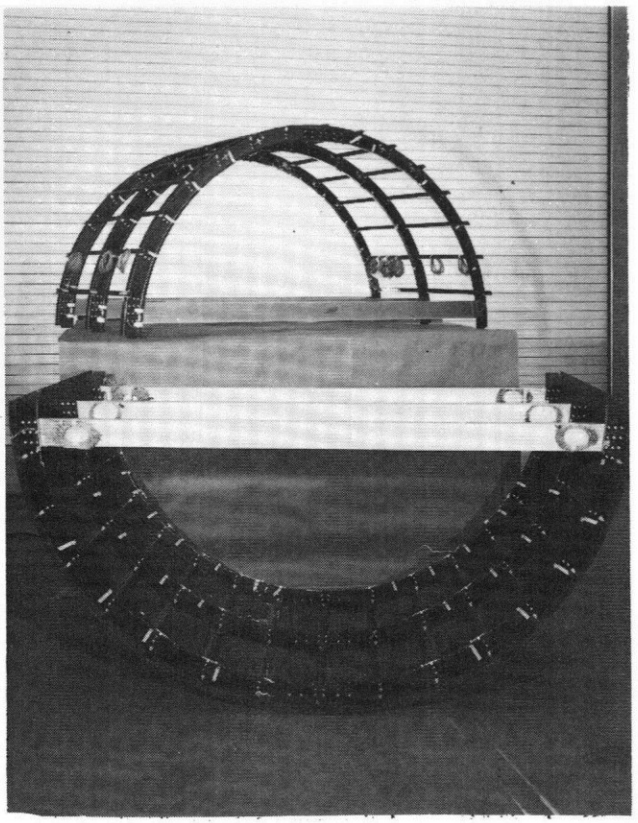

Figure 7. - Composite subfloor sections (skeleton/unskinned (top), skinned (bottom)).

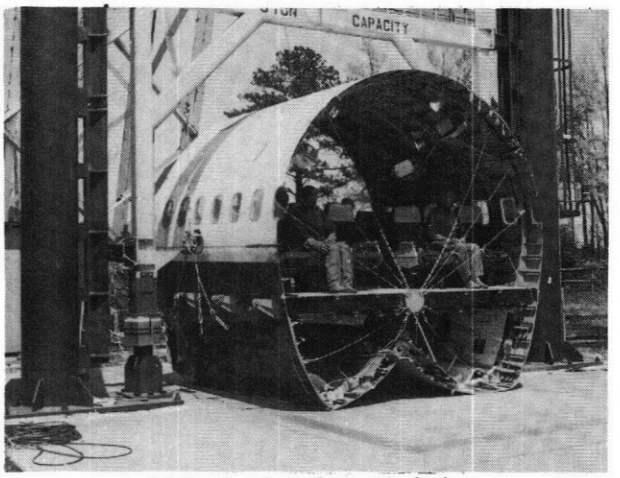

(a) Section from forward of wing.

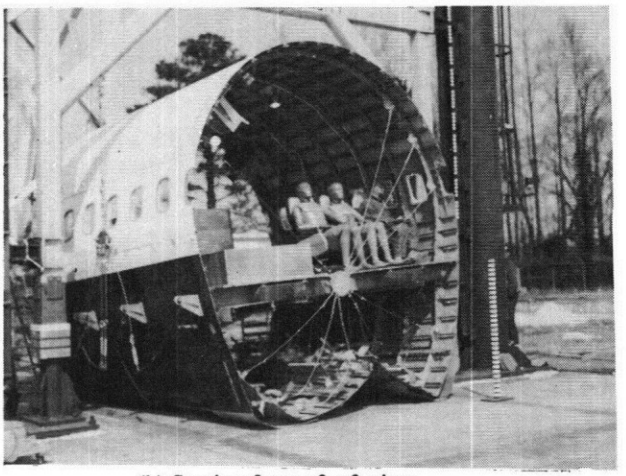

(b) Section from aft of wing.

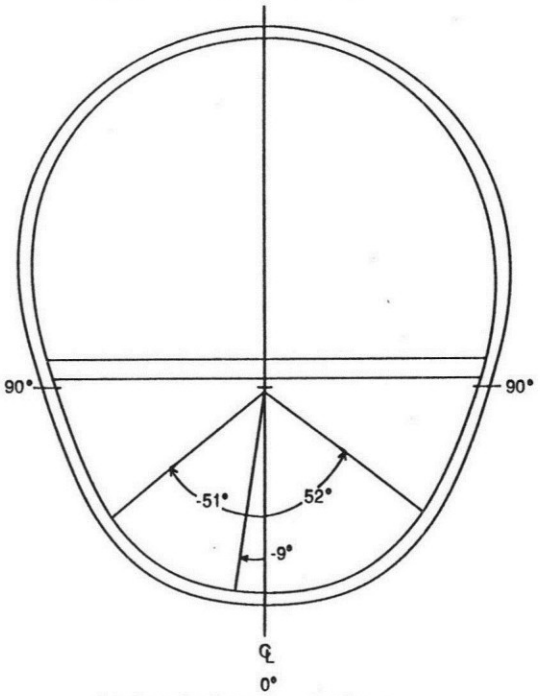

(c) Angular location of failures.

Figure 8. - Structural damage to metal aircraft structures resulting from impact tests.

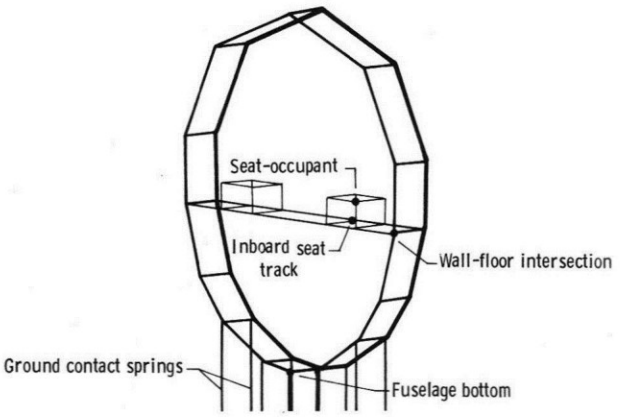

Figure 9. - Finite element two-frame model of metal transport section.

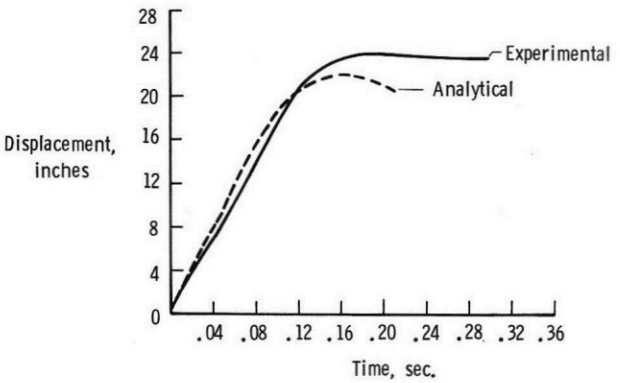

(a) Vertical floor displacement.

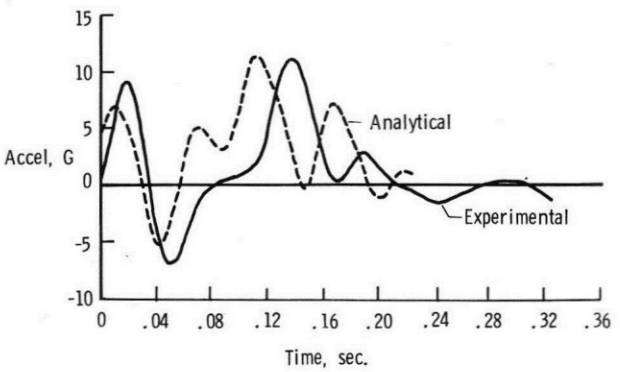

b) Vertical accelerations at wall/floor interface.

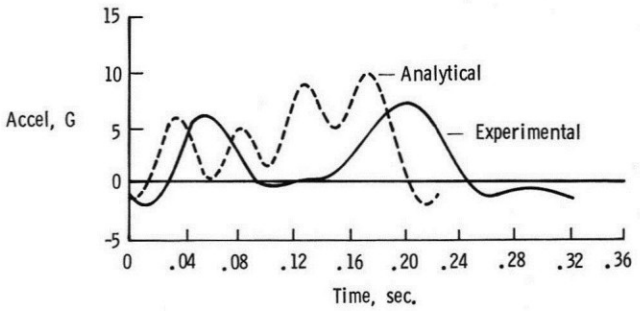

(c) Vertical pelvis acceleration.

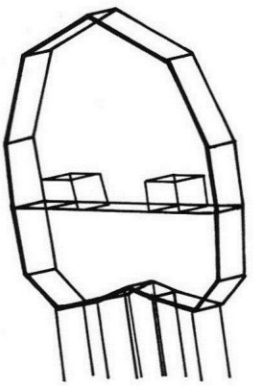

(d) Deformed model.

Figure 10. - Comparison of experimental and analytical fuselage crushing and accelerations of metal transport section.

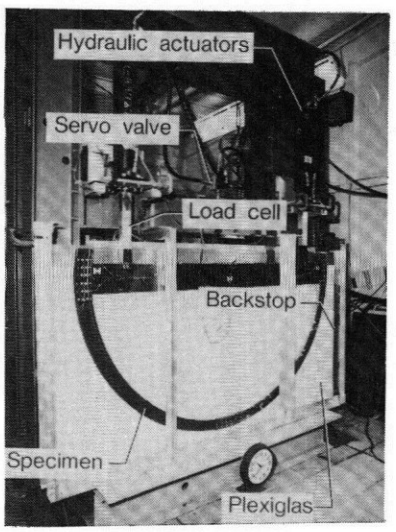

(a) Static test apparatus.

Figure 11. - Static results from tests of single composite Z-frame.

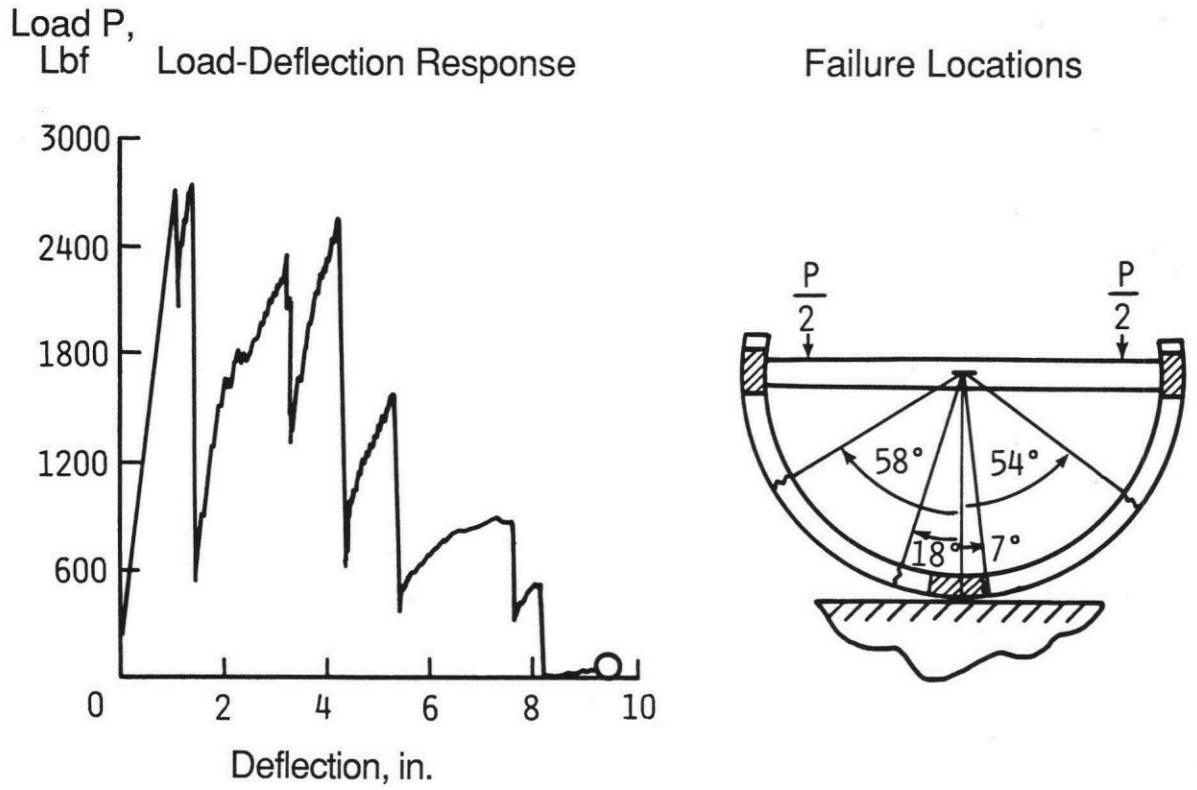

(b) Load-displacement and failure locations.

Figure 11. - Continued.

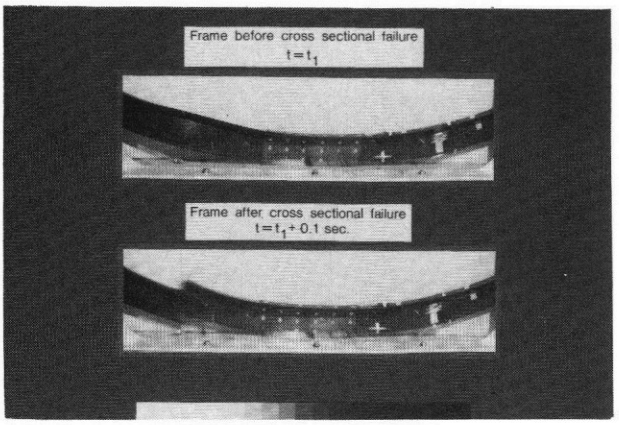

(c) Frame local instability.

Figure 11. - Concluded.

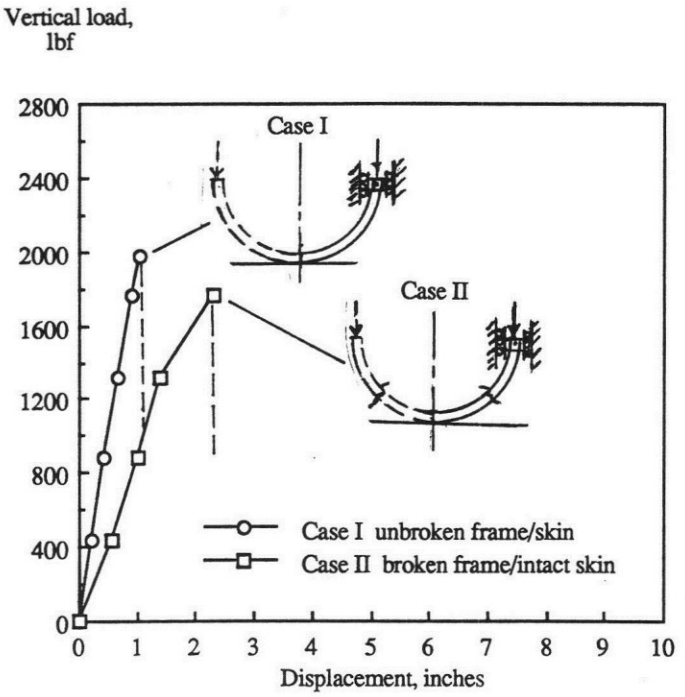

(a) Load-displacement.

Figure 12. - Typical analytical results for composite frame skin using I-section for ease of analysis.

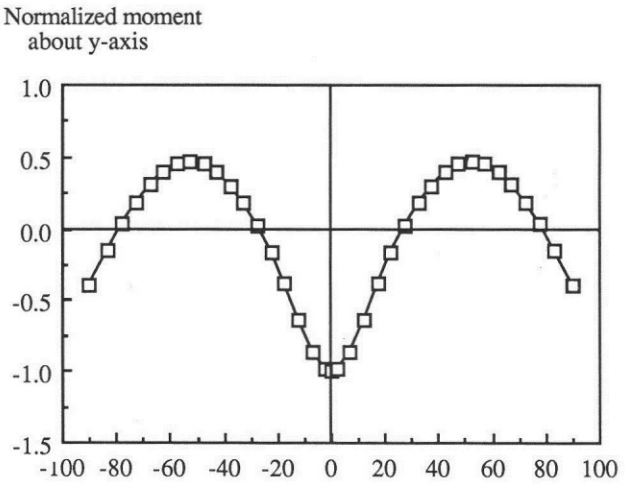

(b) Case I----Normalized moment (Prior to failure).

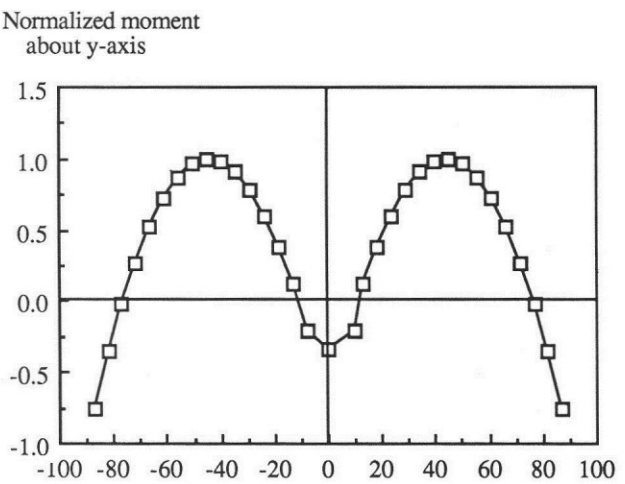

(c) Case II---Normalized moment (Broken frame-intact skin).

Figure 12. - Concluded.

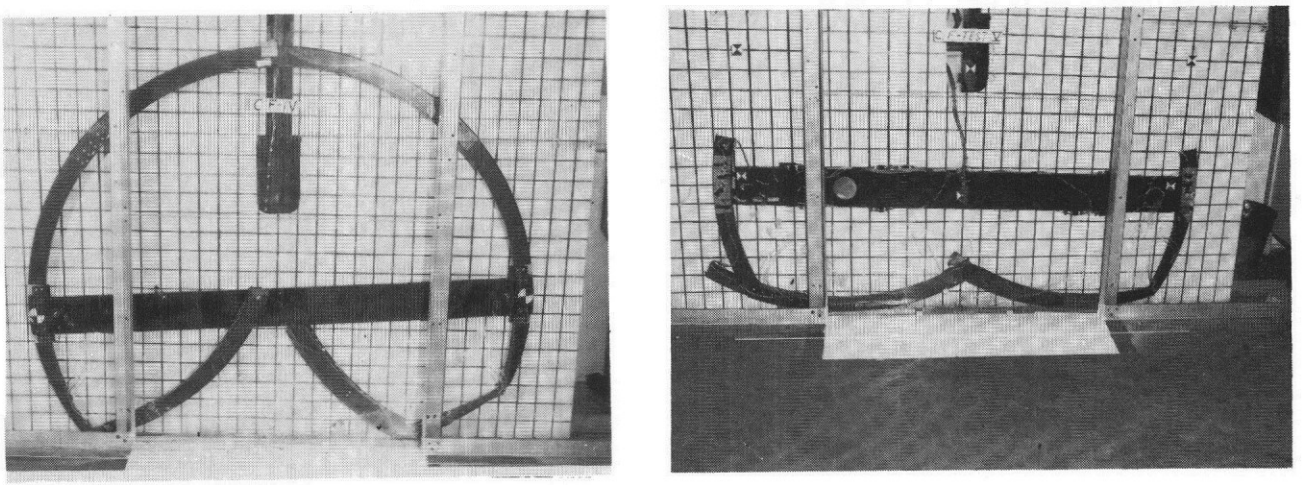

(a) Photographs of failed frames.

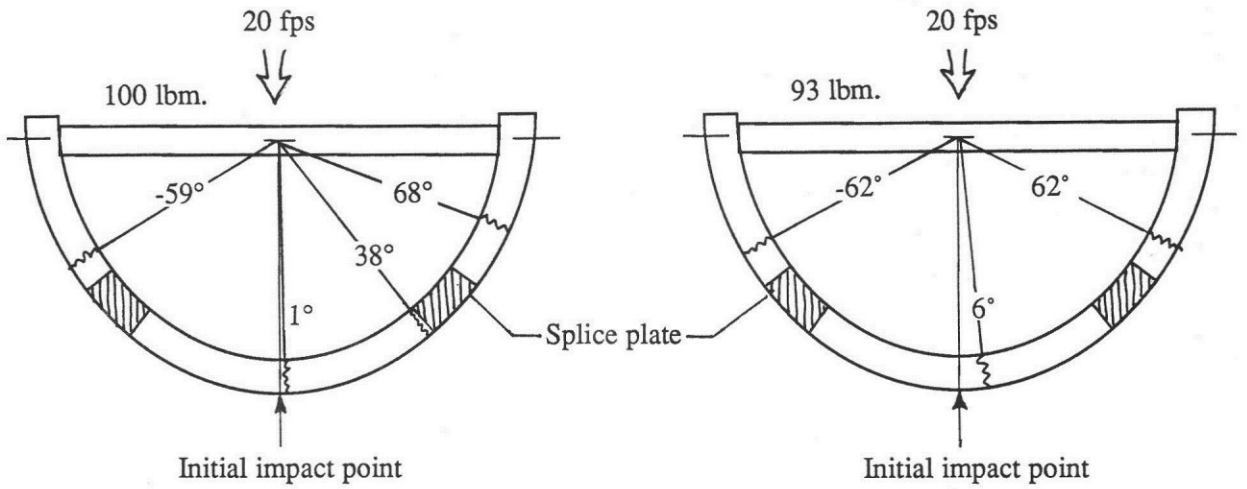

(b) Location of failures in frames.

Figure 13. - Behavior of composite Z-frame under impact loading.

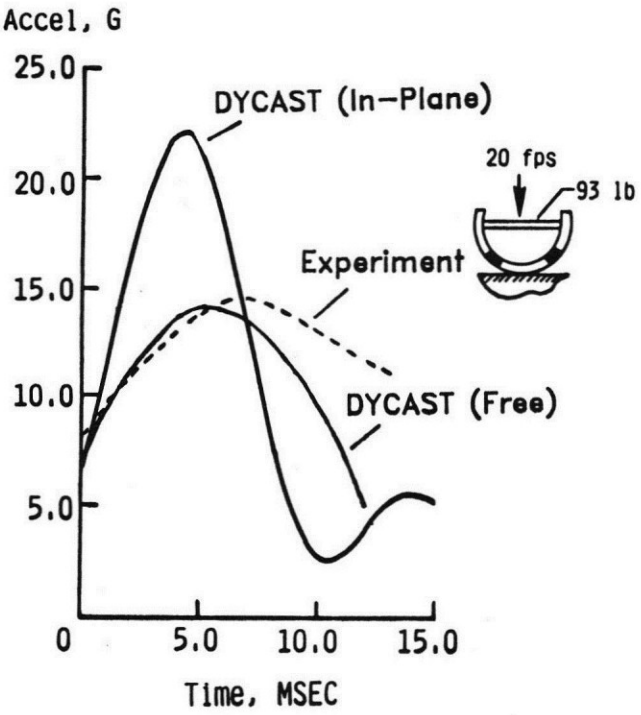

(c) Experimental and analytical accelerations.

Figure 13. - Concluded.

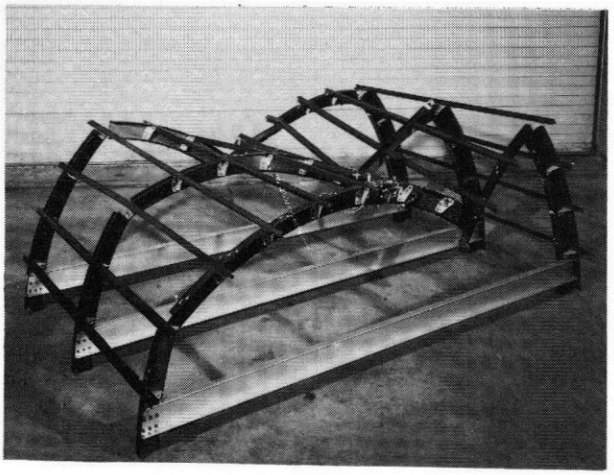

(a) Failed composite skeleton subfloor.

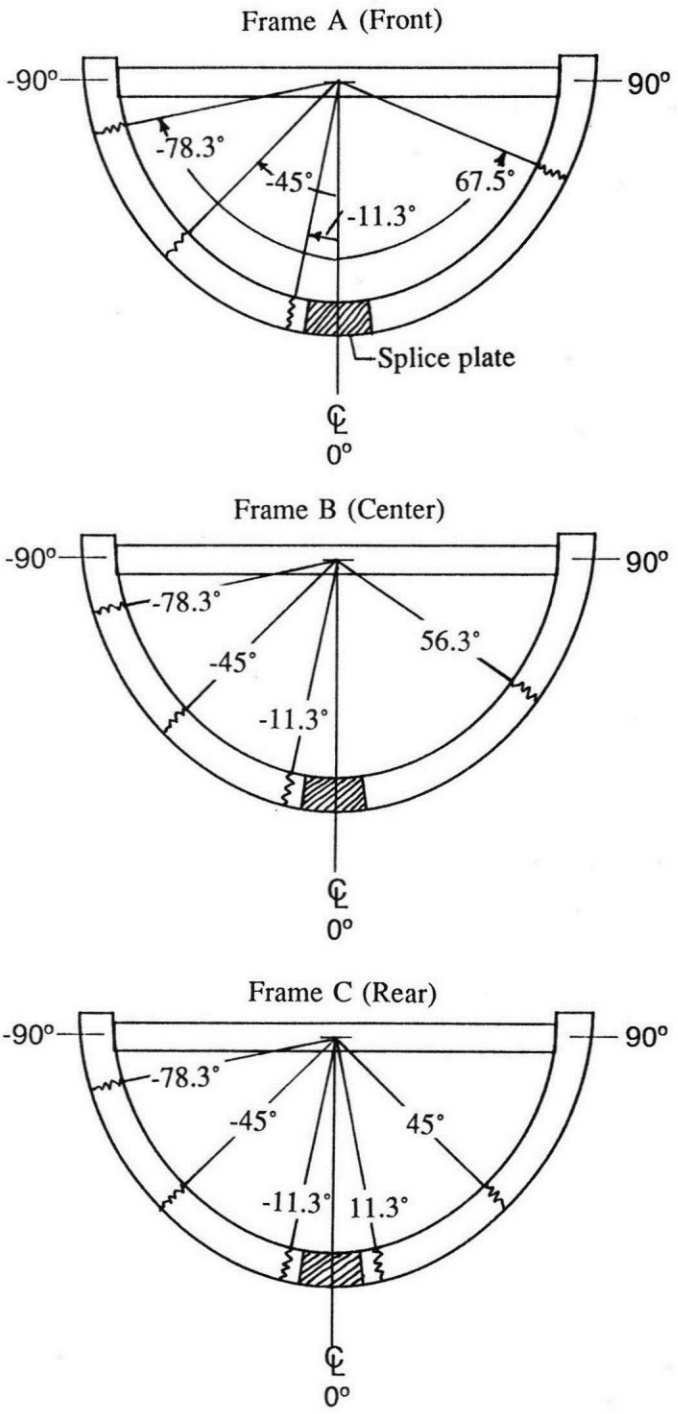

(b) Failure locations.

Figure 14. - Behavior of composite skeleton subfloor under static loading tests.

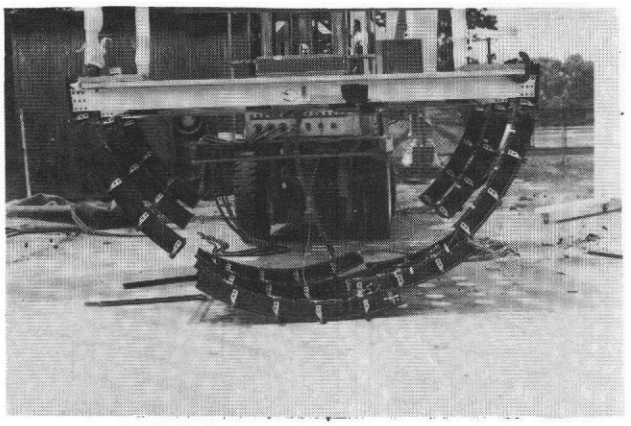

(a) Failed composite skeleton subfloor.

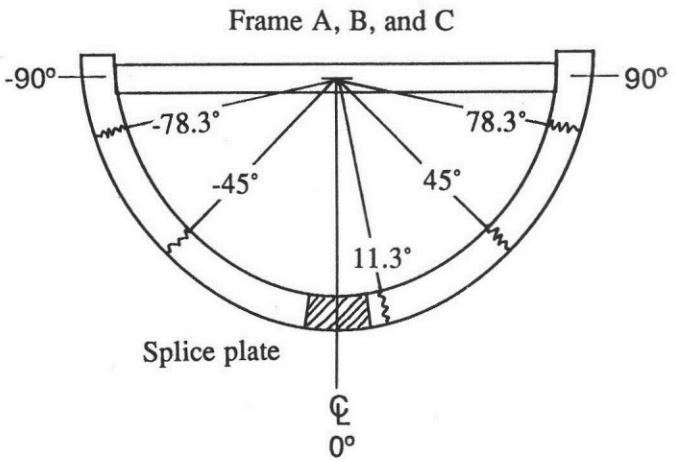

(b) Failure locations.

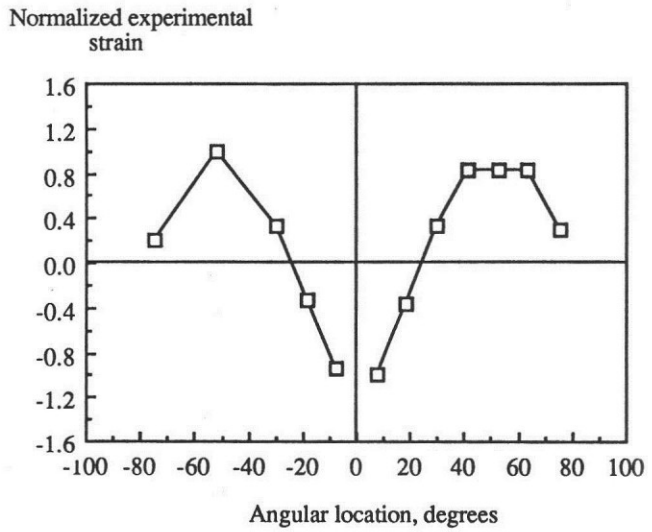

(c) Normalized circumferential strain distribution.

Figure 15. - Behavior of composite skeleton subfloor under dynamic loading tests.

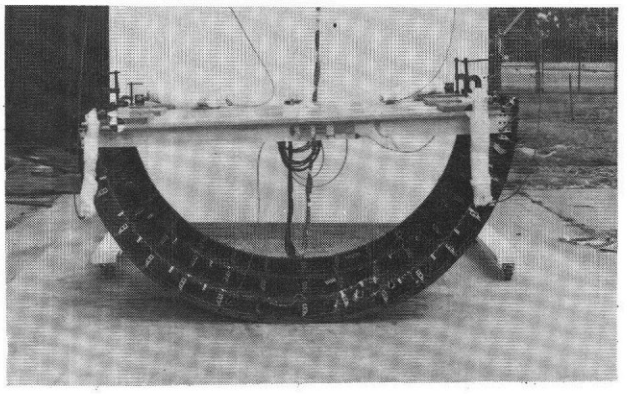

(a) Failed composite skinned subfloor.

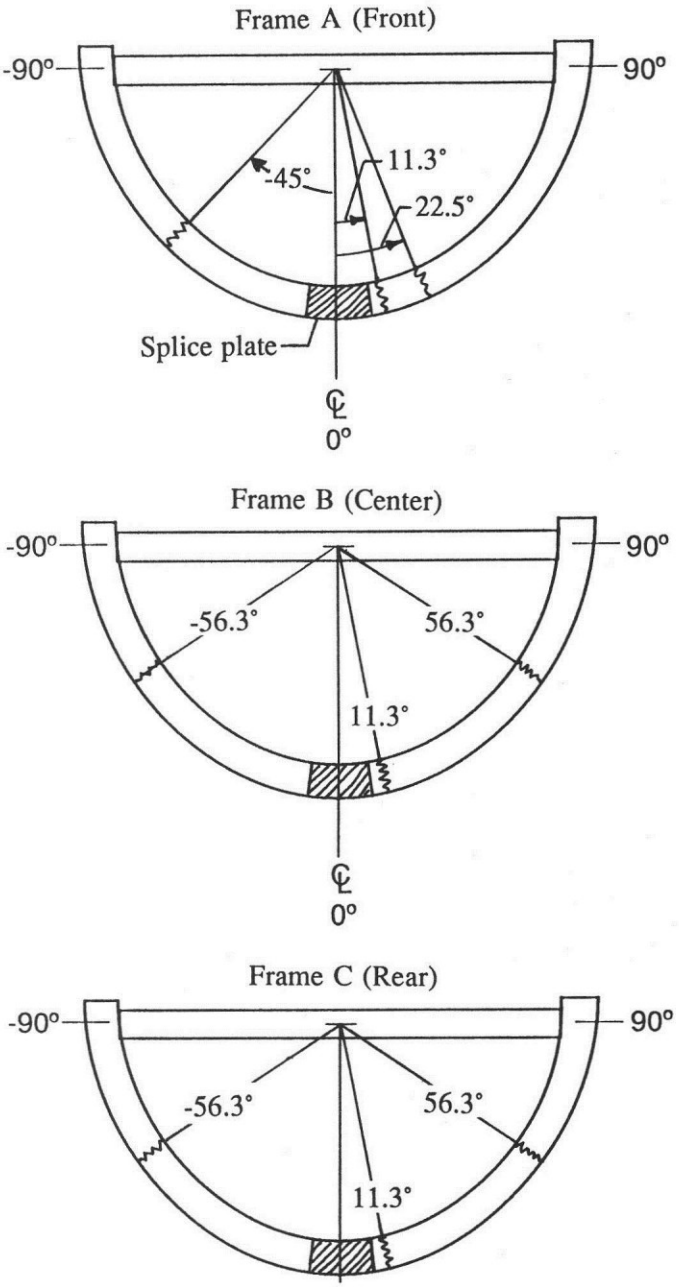

(b) Location of failures.

Figure 16. - Behavior of composite skinned subfloor under dynamic loading tests.

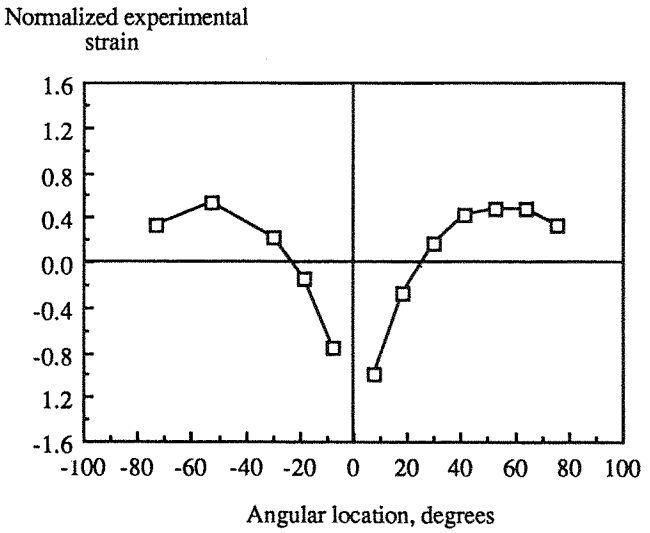

(c) Normalized circumferential strain distribution.

Figure 16. - Concluded.

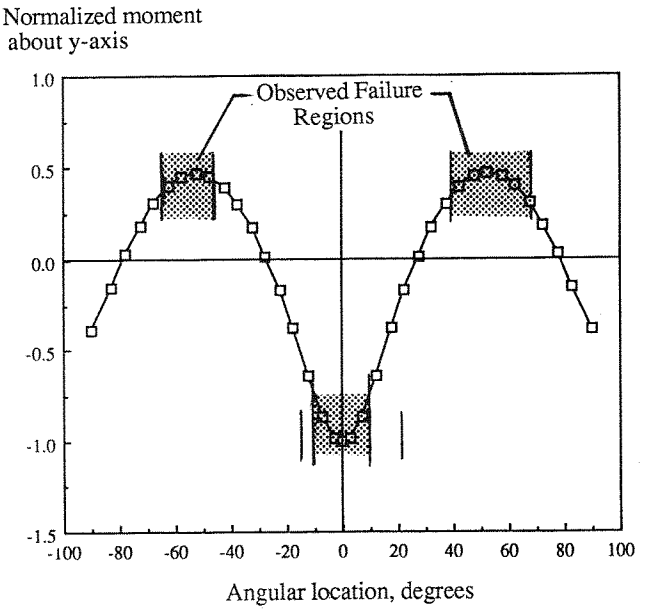

(a) Normalized moment distribution.

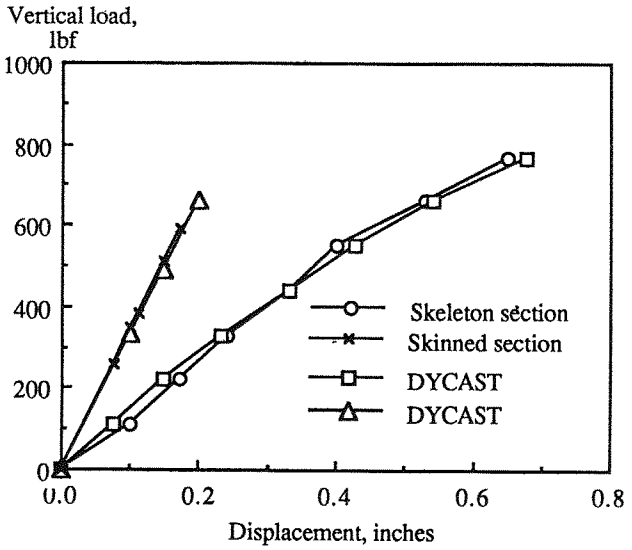

Figure 17. - Comparison of experimental and analytical stiffness of composite skeleton and skinned subfloors.

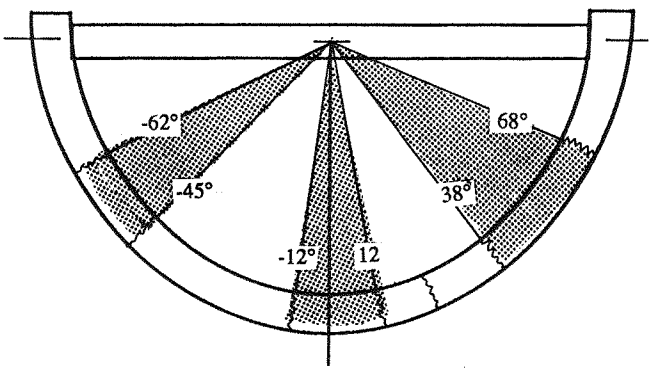

(b) Failure locations.

Figure 18. - Comparison of non-dimensional analytical moment distribution predicted by finite element frame model and observed failure locations on metal and composite fuselage components and structures.